Metal−Oxide−Semiconductor-Structured MgZnO Ultraviolet Photodetector with High Internal Gain

H. Zhu,[†,‡] C. X. Shan,*[,†] L. K. Wang,[†,‡] J. Zheng,[†,‡] J. Y. Zhang,[†] B. Yao,[†] and D. Z. Shen[†]

Key Laboratory of Excited State Processes, Changchun Institute of Optics, Fine Mechanics and Physics, Chinese Academy of Sciences, Changchun 130033, China, and Graduate School of Chinese Academy of Sciences, Beijing 100049, China

Received: February 4, 2010; Revised Manuscript Received: March 13, 2010

A Au/MgO/MgZnO metal−oxide−semiconductor-structured photodetector was fabricated. The responsivity of the photodetector was about 2 orders of magnitude larger than that of the Au/MgZnO metal−semiconductor-structured photodetector fabricated under the same procedure except that no MgO layer was introduced. The detectivity of the photodetector is about 1 order of magnitude larger than the corresponding value of Si photodetector that is widely employed for ultraviolet detection currently. The enhanced responsivity was attributed to the carrier multiplication occurring in the MgO layer via impact ionization. The results reported in this paper may provide a facile route to ultraviolet photodetectors with high internal gain.

Introduction

Ultraviolet (UV) photodetectors have a wide range of commercial applications, such as flame sensing, missile detection, communications, and medical diagnostics, etc.[1] Compared with UV-enhanced Si photodiodes or photomultiplier tubes that are widely employed as UV detectors currently, photodetectors based on wide band gap semiconductors have the advantages of smaller size, higher breakdown field, filter-free visible-blind or solar-blind UV detection, higher radiation-resistance, and wider operational temperature range.[2−4] As an important wide band gap semiconductor, zinc oxide (ZnO) has been studied extensively in recent years for its potential application in UV photodetectors, and ZnO-based photodetectors with various structures including metal−semiconductor−metal (MSM),[5−7] Schottky,[8−10] and p−n junction have been reported.[11,12] Among these types of UV photodetectors, the MSM photodetector has been highlighted for its ease of fabrication and possible monolithical integration with preamplifiers. However, the relatively large dark current and low quantum efficiency in MSM photodetectors will impede their further development towards practical applications. Generally speaking, photodetectors based on p−n junctions usually have relatively high internal gain, high sensitivity, and low noise. However, p-type doping of ZnO-based materials is still a huge challenge currently, which hinders the fabrication of ZnO-based p−n junction photodetectors.[13] For the aforementioned reasons, no report on ZnO-based UV photodetectors with internal gain can be found in the literature to the best of our knowledge. Actually, realizing ZnO-based UV photodetectors with high internal gain in a relatively simple approach has been eagerly desired for their significance and importance in the future development of this kind of photodetectors.

In this paper, a Au/MgO/MgZnO metal−oxide−semiconductor (MOS)-structured photodetector has been constructed. The introduction of MgO dielectric layer led to efficient internal gain through an impact ionization process, and the origin of the internal gain has been discussed in detail.

Experimental Methods

The MgZnO film employed as the active layer of the photodetector was prepared on sapphire substrate in a metal−organic chemical vapor deposition technique. The precursors used for the MgZnO growths were bis(cyclopentadienyl)Mg, diethylzinc, and high purity (99.999%) oxygen, and nitrogen was used as a carrier gas. The growth temperature was fixed at 550 °C, and the pressure in the growth chamber at 150 torr during the growth process. After the growth of the MgZnO film, a MgO film was deposited onto the MgZnO film in a magnetron sputtering technique. To construct a MOS- structured photodetector, a thin Au contact (about 20 nm) was deposited onto the MgO layer, and a ring-shaped Al contact onto the MgZnO film by vacuum evaporation. For comparison, another photodetector was also prepared in the same procedure with the MOS photodetector except that the MgO layer was absent, which will be named metal−semiconductor (MS) photodetector in the following text. The electrical properties of the films were characterized employing a Hall measurement system (LakeShore 7707). The composition of the MgZnO films was determined by X-ray photoelectron spectroscopy (XPS). The absorption spectrum of the MgZnO films was measured in a Shimadzu UV-3101PC scanning spectrophotometer. The response of the photodetectors was measured in a SPEX scanning monochromator employing a 150 W Xe lamp as the illumination source under front illumination conditions.

Results and Discussion

The Mg content in the MgZnO film determined by X-ray photoelectron spectroscopy is 18%, and the as-grown MgZnO film shows n-type conduction with an electron concentration of 2.0×10^{17} cm^{-3} and a mobility of 3 cm^2 V^{-1} S^{1-}. Figure 1 shows the absorption spectrum of the MgZnO film. It is clear from the spectrum that the MgZnO film shows an obvious absorption peak at 348 nm, which corresponds to the excitonic absorption of the MgZnO, for its position (3.58 eV) is reasonably

* To whom correspondence should be addressed. E-mail: phycxshan@yahoo.com.cn.
† Changchun Institute of Optics, Fine Mechanics and Physics, Chinese Academy of Sciences.
‡ Graduate School of Chinese Academy of Sciences.

10.1021/jp101083n
Published on Web 03/26/2010

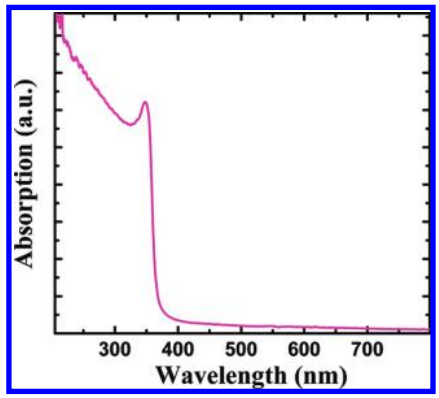

Figure 1. Room temperature absorption spectrum of the MgZnO film.

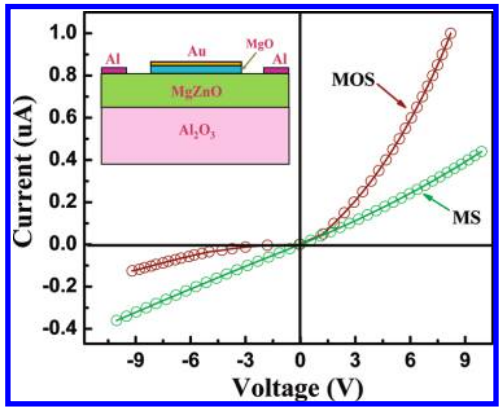

Figure 2. Current−voltage (I−V) characteristics of the MOS and MS photodetectors under dark conditions. A schematic diagram of the Au/MgO/MgZnO MOS photodetector is shown in the inset.

close to the band gap of $Mg_{0.18}Zn_{0.82}O$ (3.68 eV).[14] As evidenced from the figure, the MgZnO film has a strong absorption in the UV region, while it is almost transparent in the visible region, which is essential for its application in high rejection ratio UV photodetectors.

The inset of Figure 2 shows the schematic illustration of the MgZnO MOS-structured photodetector. The thickness of the n-type $Mg_{0.18}Zn_{0.82}O$, MgO layer, and Au contact is 350, 30, and 20 nm, respectively. The Au electrode on the MgO layer was patterned into a circular pad with the diameter of 5 mm using a shadow mask. An Al ring electrode was chosen as the contact to the MgZnO film. The current−voltage (I−V) characteristics of the MOS and MS photodetectors under dark conditions are illustrated in Figure 2. As shown in the figure, the dark current of the MOS photodetector is only 1/3 of the corresponding value of the MS photodetector under reversed bias. However, the dark current of the MOS photodetector under forward bias is obviously larger than that of the MS one, the reason for which will be detailed in the following text.

Figure 3 shows a characteristic photoresponse spectrum of the MOS photodetector at 5 V bias; for comparison, the response spectrum of the MS photodetector at 5 V bias is also shown. A response peak appears at about 366 nm for the MOS photodetector, and the maximum responsivity is 0.055 A/W, while for the MS photodetector, the position of the response peak is almost identical with the MOS one, but its responsivity (6×10^{-4} A/W) is about 2 orders of magnitude smaller than the corresponding value of the MOS photodetector. The inset shows the spectral responsivity of the MOS photodetectors at 0 V bias. One can see that at 0 V bias, obvious photoresponse can be observed for the MOS photodetector while the response of the MS

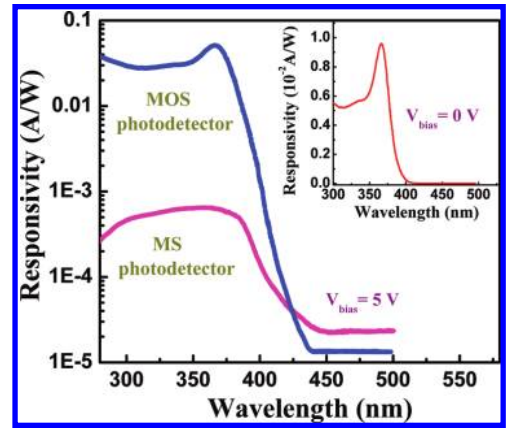

Figure 3. Spectral responsivity of the MgZnO-based MS and MOS photodetectors at 5 V bias. The inset shows the spectral responsivity of the MOS photodetector at 0 V bias.

photodetector is undetectable. The maximum responsivity of the MOS photodetector at 0 V bias is about 0.011 A/W. The thermal-noise-limited detectivity D^* of a photodetector can be expressed by the following formula[15]

$$D^* = R_\lambda (R_0 A/4KT)^{1/2} \tag{1}$$

where R_λ and R_0 are the responsivity of the photodetector and the dark impedance at 0 V bias, respectively, and A is the detector area. The detectivity D^* of the MOS photodetetor is determined to be 1.26×10^{13} cm $Hz^{1/2}$/W, which is much higher than the corresponding value of Si photodetector ($\sim 10^{12}$ cm $Hz^{1/2}$/W) that is usually employed for UV detection currently.[16] We think the high detectivity is a result of the relatively high responsivity and low dark current. Another important figure of merit of a photodetector is its noise-equivalent power (NEP), i.e., the minimum impinging optical power that a photodetector can distinguish from the noise. The NEP of a photodetector can be determined by the following expression[17]

$$\mathrm{NEP} = \frac{A^{1/2}B^{1/2}}{D^*} \tag{2}$$

where A is the detector area and B is the bandwidth. Based on the above formula, the NEP of the MOS photodetector is determined to be 4.2×10^{-13} W/$Hz^{1/2}$.

The responsivity of the MOS and MS photodetector as a function of the applied bias is illustrated in Figure 4. It is found that the responsivity of the MS photodetector shows a linear dependence on the applied bias. Such behavior is a typical characteristic of the MS photoconductive photodetectors.[3,7] Nevertheless, the responsivity of the MOS photodetector increases exponentially with increasing applied bias, indicating the existence of optical gain. The external quantum efficiency of the photodetector is given by[17]

$$\eta = \frac{I_p/e}{P_{opt}/h\nu} \tag{3}$$

where I_p is the photogenerated current with the absorption of incident optical power P_{opt} at a wavelength λ (corresponding to a photon energy $h\nu$). At 5 V bias, the external quantum efficiency of the MOS and MS structures determined from eq

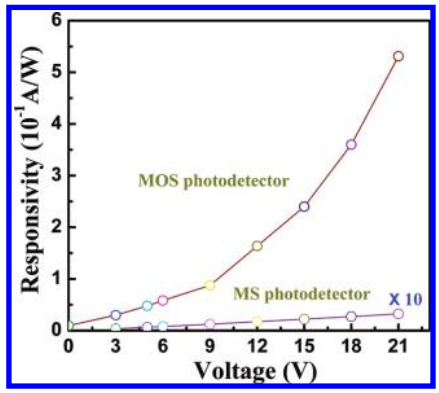

Figure 4. Responsivity of the MOS and MS photodetectors as a function of the applied bias. Note that the responsivity of the MS photodetector has been magnified by 10 times.

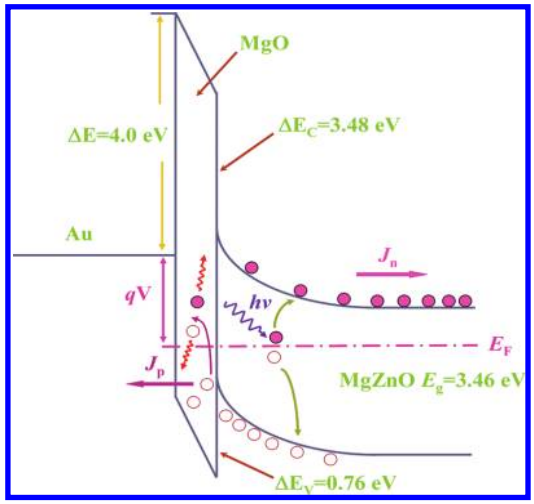

Figure 5. Schematic band gap alignment of the Au/MgO/MgZnO structure under reverse bias showing the occurrence of carrier multiplication via the impact ionization process.

3 is 22% and 0.26%, respectively. It is noteworthy that the η of the MOS photodetector increases to 200% at 21 V bias. This remarkable characteristic reveals that there is relatively high inherent photocurrent gain in the MOS structure.

In order to explore the origin of the inherent photocurrent gain, the band alignment of the Au/MgO/MgZnO structure under reverse bias is illustrated in Figure 5. The work function of Au and the electron affinity of MgO are 4.8 and 0.8 eV, respectively. Thus the barrier between the Au and MgO is 4.0 eV. Due to this large barrier, the electrons in the Au will be blocked and very few can inject into the MgZnO at reverse bias. Consequently, the dark current of the MOS structure under reverse bias is much smaller than that of the MS structure. While at forward bias, many electrons in the MgZnO layer will be concentrated at the MgO/MgZnO interface due to the large conduction band offset (3.48 eV) between the MgO and MgZnO. Consequently, high density two-dimensional electron gas (2DEG) will be formed underneath the MgO dielectric film. The 2DEG channel will decrease the transverse resistance between the Au and Al electrode strongly. As a result, the dark current of the MOS structure under forward bias is significantly larger than that of the MS structure, as shown in Figure 2. Under the illumination of the excitation source, electron−hole pairs will be generated in the MgZnO layer. At reverse bias, the generated electrons will be collected by the Al electrode, while for holes, they will transfer in a reverse pathway under the drift of the applied bias. It is rational to speculate that most of the voltage will be applied onto the MgO layer due to its dielectric nature. Therefore, the conduction and valence bands of MgO will bend significantly. Consequently, the effective thickness of the barrier that prevents holes tunneling from the MgZnO layer to the Au electrode will be reduced, and holes can tunnel through the barrier efficiently.[18] Meanwhile, the electric field in the MgO will be as high as 1.7×10^6 V/cm at 5 V bias considering that the thickness of the MgO layer is only about 30 nm. Under such a high electric field, the holes that tunnel through the MgO layer will gain much kinetic energy, and they will impact with the lattice of MgO, and some electrons in the valence band of MgO will be excited. In this way, additional carriers are generated via this impact ionization process.[19] The generation of carriers via impact ionization process has been detailed in our previous publication.[20,21] Under the drive of the bias, the excited electrons will enter into the MgZnO layer and the holes will be collected by the Au electrode. Due to the carrier multiplication process, the responsivity of the MOS-structured photodetector is increased. More carriers will be generated via the impact ionization process at larger bias, and as a result, the responsivity of the MOS photodetector increases exponentially with increasing bias. For the MS photodetector, such a carrier multiplication process is absent, and thus its responsivity increases linearly with the applied bias, as shown in Figure 4.

Conclusions

In summary, a MgZnO-based MOS-structured UV photodetector with high internal gain has been constructed, and the responsivity of the device is about 2 orders of magnitude larger than that of the MS photodetector fabricated under the same procedure except that no MgO dielectric layer is introduced. The detectivity of the photodetector can reach 1.26×10^{13} cm $Hz^{1/2}$/W, almost 1 order of magnitude larger than that of Si photodetectors that are widely employed for UV detection currently. The improved responsivity has been attributed to the carrier multiplication process occurring in the MgO layer via impact ionization. The results reported in this paper provide a facile route to ZnO-based UV photodetectors with high internal photocurrent gain and thus may lay a solid ground for the future applications of this kind of photodetectors.

Acknowledgment. This work is supported by the Knowledge Innovation Program of the CAS (no. KJCX3.SYW.W01), the "973" program (no. 2008CB317105), the Natural Science Foundation of China (nos. 10774132, 10974197, and 60976040), and the Instrument Developing Project of Chinese Academy of Sciences (YZ200903).

References and Notes

(1) Razeghi, M.; Rogalski, A. *J. Appl. Phys.* **1996**, *79*, 7433.
(2) Zhang, Y.; Shen, S. C.; Kim, H. J.; Choi, S.; Ryou, J. H.; Dupuis, R. D.; Narayan, B. *Appl. Phys. Lett.* **2009**, *94*, 221109.
(3) Yang, W.; Vispute, R. D.; Choopun, S.; Sharma, R. P.; Venkatesana, T. *Appl. Phys. Lett.* **2001**, *78*, 2787.
(4) Liao, M. Y.; Koide, Y.; Alvarez, J. *Appl. Phys. Lett.* **2007**, *90*, 123507.
(5) Yang, W.; Hullavarad, S. S.; Nagaraj, B.; Takeuchi, I.; Sharma, R. P.; Venkatesan, T.; Vispute, R. D.; Shen, H. *Appl. Phys. Lett.* **2003**, *82*, 3424.
(6) Ryu, Y. R.; Lee, T. S.; Lubguban, J. A.; White, H. W.; Park, Y. S.; Youn, C. J. *Appl. Phys. Lett.* **2005**, *87*, 153504.
(7) Ju, Z. G.; Shan, C. X.; Jiang, D. Y.; Zhang, J. Y.; Yao, B.; Zhao, D. X.; Shen, D. Z.; Fan, X. W. *Appl. Phys. Lett.* **2008**, *93*, 173505.
(8) Endo, H.; Sngibuchi, M.; Takahashi, K.; Goto, S.; Sugimnra, S.; Hane, K.; Kashiwaba, Y. *Appl. Phys. Lett.* **2007**, *90*, 121906.
(9) Endo, H.; Kikuchi, M.; Ashioi, M.; Kashiwaba, Y.; Hane, K.; Kashiwaba, Y. *Appl. Phys. Express.* **2008**, *1*, 0512011.

(10) Jiang, D. Y.; Shan, C. X.; Zhang, J. Y.; Lu, Y. M.; Yao, B.; Zhao, D. X.; Zhang, Z. Z.; Fan, X. W.; Shen, D. Z. *Cryst. Growth Des.* **2009**, *9*, 454–456.

(11) Liu, K. W.; Shen, D. Z.; Shan, C. X.; Zhang, J. Y.; Yao, B.; Zhao, D. X.; Lu, Y. M.; Fan, X. W. *Appl. Phys. Lett.* **2007**, *91*, 201106.

(12) Ohta, H.; Hirano, M.; Nakahara, K.; Maruta, H.; Tanable, T.; Kamiya, M.; Kamiya, T.; Hosono, H. *Appl. Phys. Lett.* **2003**, *83*, 1029.

(13) Look, D. C.; Claflin, B.; Alivov, Ya. I.; Park, S. J. *Phys. Status Solidi A* **2004**, *201*, 2203–2212.

(14) Chen, J.; Shen, W. Z.; Chen, N. B.; Qiu, D. J.; Wu, H. Z. *J. Phys.: Condens. Matter* **2003**, *15*, L475–L482.

(15) Donati, S. *Devices, Circuits, and Applications*; Prentice Hall: Upper Saddle River, NJ, 2000.

(16) Gong, X.; Tong, M.; Xia, Y.; Cai, W.; Moon, J. S.; Cao, Y.; Yu, G.; Shieh, C. L.; Nilsson, B. A.; Heeger, J. *Science* **2009**, *325*, 1665–1667.

(17) Sze, S. M. *Physics of Semiconductor Devices*, 2nd ed.; John Wiley: New York, 1981.

(18) Zhu, H.; Shan, C. X.; Yao, B.; Li, B. H.; Zhang, J. Y.; Zhang, Z. Z.; Zhao, D. X.; Shen, D. Z.; Fan, X. W.; Lu, Y. M.; Tang, Z. K. *Adv. Mater.* **2009**, *21*, 1613–1617.

(19) Hudgins, J. L.; Simin, G. S.; Santi, E.; Khan, M. A. *IEEE Trans. Power Electron.* **2003**, *18*, 907–914.

(20) Zhu, H.; Shan, C. X.; Zhang, J. Y.; Li, B. H.; Zhao, D. X.; Z. Z.; Zhang, Yao, B.; Shen, D. Z.; Fan, X. W.; Tang, Z. K.; Hou, X. H.; Choy, K. L. *Adv. Mater.* DOI: 10.1002/adma.200903623.

(21) Wang, W. J.; Shan, C. X.; Zhu, H.; Ma, F. Y.; Shen, D. Z.; Fan, X. W.; Choy, K. L. *J. Phys. D: Appl. Phys.* **2010**, *43*, 045102.

JP101083N